Diffusion of helium in the perfect uranium and thorium dioxide single crystals

Ludwik Dąbrowski,
Marcin Szuta

Abstract. We present quantum-mechanical evaluation of helium diffusion coefficient in the crystalline UO_2 and ThO_2. Parameters assignment of Schrödinger's equation were done using the crystal field potentials which were obtained applying the density functional theory (DFT). "Ab initio" calculations were performed using the Wien2k program package. To compute the unit cell parameters the 13 atom super-cell was chosen. Applying two-site model we evaluated the time for an over-barrier jump and diffusion of interstitial He. The obtained values for diffusion coefficient are compared with the experimentally obtained values and with the theoretical values of other authors. In addition, it is simultaneously shown that helium diffusion in these materials is a quantum diffusion.

Key words: uranium • thorium dioxide • diffusion • tunneling • DFT+U • generalized gradient approximation (GGA) • potential barrier • incorporated helium

L. Dąbrowski✉, M. Szuta
National Centre for Nuclear Research (NCBJ),
7 Andrzeja Sołtana Str., 05-400 Otwock/Świerk, Poland,
Tel.: +48 22 718 0155, Fax: +48 22 779 3888,
E-mail: luddab@hotmail.com

Introduction

It is a well known accumulation ability of huge amount of helium by UO_2 and ThO_2 crystals during several billions of years in their minerals. Similar phenomena of helium accumulation occurs in the nuclear fuel under irradiation where helium is produced as a result of the alpha decay of certain actinides. Initially it was considered, although helium is the noble gas, that a weak chemical bonding can be induced in the environment of heavy atoms.

The first attempt of explanation of the helium incorporation in UO_2 crystal was undertaken in the early 1990s [11]. It was estimated the bond energy of helium atoms in the uranium dioxide crystal equal to –0.1 eV. As the result was negative, so the helium atom could be permanently chemically bond in the uranium dioxide crystal.

The later study using the density functional theory (DFT)-generalized gradient approximations (DFT-GGA) [3, 12] frame-work – did not confirm this result. The obtained results of bond energies lying in the range from +0.77 to +1.83 eV exclude the ability of chemical bond.

In Ref. [7] another approach of the issue was presented. Instead of chemical bond – the helium atom immobilization in a deep potential well inside the crystallographic lattice was proposed. To solve the issue "ab initio" Wien2k [2] program packages were used. The methods estimate the energy barrier between interstitial sites in perfect lattice UO_2 + He on about

8 eV. We have shown there that in these circumstances the helium atom creates local bond state and performs oscillation of small amplitude, so the probability of over barrier jump to neighbour interstitial site, and hence the diffusion coefficient are close to zero.

The height of the potential barrier between interstitial sites in perfect lattice was evaluated in [11], which appeared to be equal to +3.8 eV. All these estimates were obtained using methods of molecular thermodynamics. Authors in Ref. [18] give two potential values 2.56 and 2.3 eV making reference to [9]. Later in this work the discrepancy will be discussed over.

Diffusion significantly favour the crystal lattice defects. In the case of UO_2, as shown by experimental results, the effect is large. Authors of Ref. [17] using ^{3}He(d,α)^{1}H Nuclear Reaction Analysis Technique, obtained for the crystalline UO_2 at a temperature of 1000°C the diffusion coefficient equal to $D = 3.7 \pm 0.74 \times 10^{-14}$ cm^2·s^{-1}, while authors of Ref. [16] applying the same method, obtained for the UO_2 matrix and the same temperature the diffusion coefficient equal once to $D = 2.9 \times 10^{-13}$ cm^2·s^{-1} and once to $D = 3.7 \times 10^{-14}$ cm^2·s^{-1} depending on the flux value.

Annealing, reducing the amount of defects, reduces the diffusion coefficient D, in other words the defects enhance the diffusion mechanism. So, for example, the authors [13] obtained the value of diffusion coefficient equal to $D = 6 \times 10^{-13}$ cm^2·s^{-1}, and in [15], after annealing at 1100°C during 25 min its value decreased below 2×10^{-14} cm^2·s^{-1}.

Although annealing at high temperatures reduce the amount of defects, it does not eliminate them. They remain at the level of equilibrium for a given temperature. According to the Gibbs distribution, the number of defects remaining in the thermodynamic equilibrium with environment, is proportional to the Boltzmann factor $-\exp(E_i/kT)$, where E_i is the energy of i-defect. Despite of the high-temperature annealing, their amount can be still substantial. For this reason, the actual value of D for a perfect crystal is always smaller than the experimental values obtained. This also applies to the above-mentioned values, obtained in [15].

The calculation of the diffusion coefficient we made applying two-site model which was for the first time used for the system UO_2 + He in [7] and we evaluated the time for an over-barrier jump. In contrast to [7] in the calculations we took into account changes in local deformation during He wandering between vacancies and its impact on the barrier height, what appeared to be significant.

Method of calculations

"Ab initio" calculations of the electronic structure were performed using the Wien2k program package [2] based on the density functional theory (DFT). The Kohn-Sham (K-S) total-energy functional is used here as follows

$$(1) \quad E[\Psi_i] = 2\sum_i \int \Psi_i^* \left(-\frac{\hbar^2}{2m}\right) \nabla^2 \Psi_i d^3\vec{r} + \int V_{ion}(\vec{r}) n(\vec{r}) d^3\vec{r}$$

$$+ \frac{e^2}{2} \iint \frac{n(\vec{r})n(\vec{r}')}{|r-r'|} d^3\vec{r}' + E_{XC}[n(\vec{r})] + E_{ion}(\{\vec{R}_i\})$$

The first term of Eq. (1) describes the kinetic energy of electrons, in the second term $V_{ion}(\vec{r})$ is the electron-ion potential and $n(\vec{r})$ is the electronic density. The third term describes the Coulomb electron-electron interaction, the fourth term $E_{XC}[n(\vec{r})]$ is the exchange-correlation energy functional and the fifth term $E_{ion}(\{\vec{R}_i\})$ is the Coulomb energy associated with interaction among the nuclei at positions $\{\vec{R}_i\}$.

Taking into consideration the above, in all DFT calculations we use several exchange-correlation energy functional $E_{XC}[n(\vec{r})]$ within the generalized gradient (GGA) approximations. All the calculation were performed using the Hubbard model (DFT+U), corrective exchange-correlation energy functional $E_{XC}[n(\vec{r})]$, namely: PBE-GGA+U.

The electron spin-polarization was taken into account.

Deformation of the crystal lattice while wandering helium atoms between octahedral sites

Compounds UO_2 and ThO_2 are isomorphic, with a face-centred cubic lattice (fcc) of the calcium fluorite type structure, with similar lattice parameters: $a = 5.396$ and 5.5975 Å [1], respectively and space group Fm-$3m$ (#225).

Helium atom located in the octahedral site causes a local increase in lattice parameters. This change is not big because of the small ionic radius of He. Thus, in the case of UO_2 + He it is only from 0.04 to 0.02 Å depending on the assumed model [12]. According to our calculations, it is at the level of 0.017 Å, which is only about 0.3% of the lattice parameter. All inter atomic distances in the crystal structure are increased exactly of this percent. As shown by our calculations oxygen atoms being closest to the He, spread additionally apart at a distance of approximately 0.00045 Å, which is negligibly small.

The uranium atoms remain in their places. Thus, the local deformation of the crystal lattice is negligible, and the effect in practice settles down to a small, local increase in lattice parameter. So, with this in mind, in [7] we assumed that the deformation of the lattice during the helium migration between the sites does not change the crystal field potential. In this paper, we decided to verify this hypothesis.

Numerical calculations show that with increasing deviation from the equilibrium state, for example, from (0, 0, 1/2), the local deformation increases, reaching a maximum at the position (1/4, 1/4, 1/2). This applies to both UO_2 and ThO_2. Taking into account the considered by us 13 atomic super-cell, the helium atom in a position (0, 0, 1/2), has in its first neighbourhood eight oxygen atoms, located at alike distances equal to $(\sqrt{3}/4)a$ while uranium atoms has 6 uranium atoms in the distance equal to $1/2a$ (first coordination shell) and 8 uranium atoms in the distance $(\sqrt{3}/2)a$ (second coordination shell). In a position (1/4, 1/4, 1/2) the situation is different. Oxygen atoms in relation to the helium can be found in the three coordination shells with radius $r_1 = 1/4a$, $r_2 = (\sqrt{5}/4)a$ and $r_3 = 3/4a$ while uranium atoms in two shells $R_1 = \sqrt{2}/4a$ and $R_2 = \sqrt{6}/4a$. The local changes of deformation in these extreme positions are shown in Table 1.

Table 1. Change of lattice parameter Δa and change of radiuses of coordination shells of oxygen and uranium or thorium atoms in relation to helium atom, which is located in the position $(1/4, 1/4, 1/2)$. Additionally in the second column, change of lattice parameter Δa in the position $(0, 0, 1/2)$ is placed

Chemical compound	$\Delta a_{(0,0,1/2)}$ (Å)	$\Delta a_{(1/4,1/4,1/2)}$ (Å)	$\Delta r_{1(1/4,1/4,1/2)}$ (Å)	$\Delta r_{2(1/4,1/4,1/2)}$ (Å)	$\Delta r_{3(1/4,1/4,1/2)}$ (Å)	$\Delta R_{1(1/4,1/4,1/2)}$ (Å)	$\Delta R_{2(1/4,1/4,1/2)}$ (Å)
UO_2 + He	0.017	0.105	0.324	0.045	0.088	0.212	0.106
ThO_2 + He	0.012	0.128	0.299	0.020	0.077	0.272	0.087

As you can see from Table 1, change of the local structure, when a helium atom is in the position $(1/4, 1/4, 1/2)$, is surprisingly large compared to these changes, when helium takes equilibrium position $(0, 0, 1/2)$. In particular, a big change on movement of the oxygen atoms in the first coordination shell r_1 – about 6% lattice parameter for UO_2 and more than 5% for ThO_2. In this site of helium atom the uranium or thorium atoms undergo significant displacements, what is not observed in the equilibrium position $(0, 0, 1/2)$.

Crystal field potential

For the adiabatic approach, we numerically determine the potential values of crystal field in UO_2 and ThO_2 along the direction of neighbour interstitial octahedral positions. As contrasted with [7], the calculations took into account, as described above, changes in the local deformation of the lattice in position $(x, x, 1/2)$ and their impact on the potential barrier height.

By **x** it is denoted the current He position $(x, x, 1/2)$ during displacement between the neighbour octahedral interstitial positions in the range from $x = 0$ to $x = 1/4$. Such a potential calculations were performed by usage of the Wien2k program package for the mentioned above all five exchange-correlation energy functional $[E_{XC}[n(\vec{r})]] + U$ approximations. The value of the correlation energy U was fixed at 4.6 eV, as suggested in Ref. [12]. In a view of periodicity of the crystal lattice (Fig. 1), the calculations were performed in the range from $(0, 0, 1/2)$ to $(1/4, 1/4, 1/2)$. The potential values $V(x)$ of the UO_2 + He and ThO_2 + He arrangement were calculated with the usage of PBE-GGA+U, potential
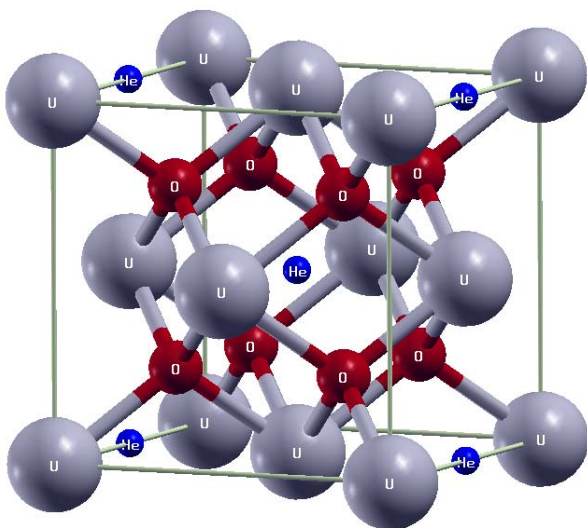
approximations. All the calculated potentials are presented in Fig. 2.

In determining the parameters for the Schrödinger equation, the potential value presented in Fig. 2 we approximated by the Gaussian curve

$$(2) \qquad V = \Delta V e^{-2\frac{(x-x_c)^2}{w^2}}$$

where ΔV – potential barrier height, x – current crystal coordinate of helium atom, $x_c = 0.25$, $w = 0.1549$.

For small x, better approximation is obtained by means of power series

$$(3) \quad V = \Delta V(8.961x^2 + 433.68518x^4 - 1905.72859x^6),$$
$$x < 0.08 \text{ for } UO_2$$

and

$$(4) \qquad V = \Delta V(14.156x^2 + 216.67x^4 - 1396.32x^6),$$
$$x < 0.08 \text{ for } ThO_2.$$

Results of potential barrier height are $\Delta V = 4.15$ eV for UO_2 + He (Fig. 2). This value is smaller than the previously obtained in [7], what is a result of local deformation of the crystal lattice, but is greater than obtained by other authors using molecular dynamics. Collected results of potential barrier height ΔV potentials for UO_2 + He and for ThO_2 + He are presented in Table 2.

Helium atom in the crystal field potential well of UO_2 and ThO_2

According to the above calculation results, the helium atom located in the octahedral interstitial position exists in a deep potential well. This suggests hypothesis that
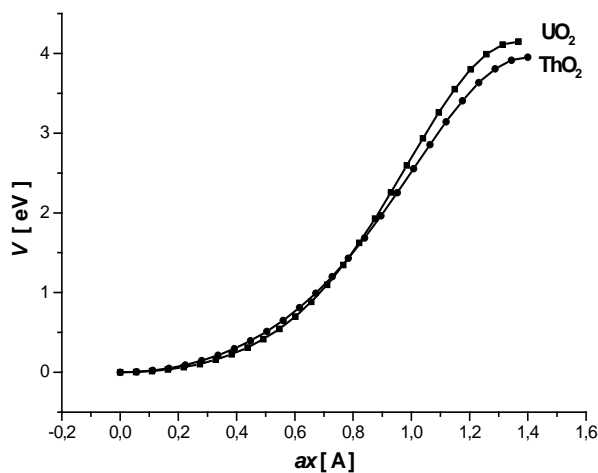

Fig. 1. The He atoms incorporation into the octahedral sites of the UO_2 lattice.

Fig. 2. Crystal field potential V vs. helium location $(x, x, 1/2)$ in the UO_2 and ThO_2 crystal lattice for the range from $ax = 0$ to $ax = 0.25$, where a denotes lattice parameter.

Table 2. Values of potential barrier height for UO_2 and ThO_2 calculated by us and other authors (ΔV values are given in eV)

Chemical compound	Ref. [7] ΔV	This work ΔV	Ref. [11] ΔV	Ref. [18] ΔV	Ref. [9] ΔV
UO_2	8.12	4.15	3.8	2.56	2.3
ThO_2	–	3.95	–	–	–

these helium atoms can form bound states in the UO_2 and ThO_2 crystal lattices.

For the above assumptions, movement of the helium atoms can be described with the Schrödinger equation in the form

$$(5) \qquad -\frac{\hbar^2}{2m}\frac{d^2}{dx^2}\Psi + V(x)\Psi = E\Psi$$

where: m – mass of helium atom, $V(x)$ – potential, E – helium atom energy.

If to develop the potential $V(x)$ into power series around the equilibrium position and neglect all terms above the second power, we get the well known harmonic oscillator approach. This eigenfunction base of harmonic oscillator can be the solution of Eq. (5) but this base is not optimal (Fig. 3). Solving Eq. (5) by using this eigenfunction, lead to the Hamiltonian matrix $H_{mn} = \langle \Psi_m | H | \Psi_n \rangle$, which is no diagonal. Using the numeric diagonalization methods and using the same Hermite polynomials as basic functions, we can find stationary values and eigenvectors. In our case we applied the Jacobi numerical methods. As the basis function for calculation the Ψ_m functions were selected, which are eigenfunctions of potential approximated with optimal parabola, at which not diagonal elements are minimized.

When temperature is not equal to absolute zero, the helium atom can occupy each energy level, but probability of such an event decreases according to the following equation

$$(6) \qquad P_n = \frac{A}{\exp(E_n / k_B T) - 1}$$

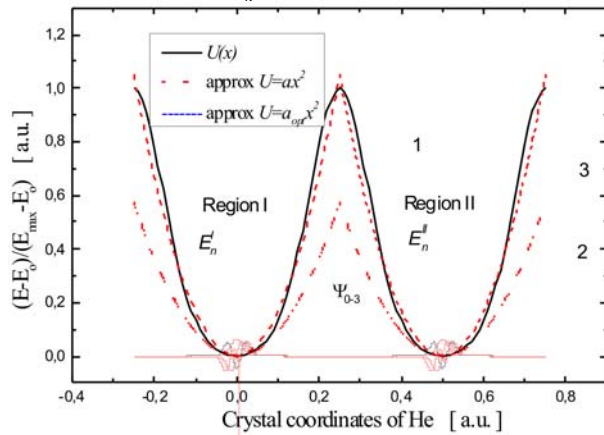where $\qquad A^{-1} = \sum_n [\exp(E_n / k_B T) - 1]^{-1}$

Fig. 3. Two-site model schema. E_0 – zero energy level of the helium atom in the octahedral interstitial position, calculated using "ab initio" method, E_n^{I}, E_n^{II} energy levels in the regions I and II, respectively, Ψ_{0-3} – first four graphs of wave functions $\Psi_n(x)$, localized in the I and II positions, 1 – potential $V(x)$, 2 – parabola approximations, 3 – optimal parabola approximations.

The thermodynamic equilibrium wave function of helium atoms is not already a pure eigenfunction, but superposition of these functions. In order to accomplish the condition (6) the thermodynamic equilibrium wave function of helium atom should get the form

$$(7) \qquad \Psi_{equilib} = p_n \Psi_n$$

where $p_n = \sqrt{P_n}$, because then the condition $\langle | \Psi_{equilib} |^2 \rangle = 1$ is accomplished at any temperature.

Overbarrier jump of helium atoms by crystal field potential barrier of UO_2 and ThO_2

Let us consider the two-site model, consisting simultaneously of the occupied (region I) and not occupied adjacent octahedral interstitial positions (region II). We believe therefore, that the helium atom has available energy levels of the two octahedral interstitial positions, but it occupies one of them. The potentials of the two positions, their parabola approximations and first four graphs of wave functions $\Psi_n(x)$, localized in the two positions are illustrated symbolically in Fig. 3. There are also symbolically marked the energy levels in both regions. Below we assess the time required for over-barrier jump in function of temperature.

If the helium atom occupies a certain energy level in the octahedral interstitial position I (Fig. 3), its state describes wave function $\Psi_{equilib}^{I}(x)$. If, on the contrary, the octahedral interstitial position II is occupied, and the position I is empty – we have an analogous situation; the arrangement is in the quantum state $\Psi_{equilib}^{II}(x)$. The wave functions of such an arrangement are analogous, but located in the second position, what is symbolized by the index II. However, the matrix elements, containing the functions $\Psi_{equilib}(x)$ from different regions are different from zero

$$(8) \qquad H_{equilib}^{I-II} = \left\langle \Psi_{equilib}^{II} | H | \Psi_{equilib}^{I} \right\rangle = H_{12} \neq 0$$

The matrix elements, containing the functions $\Psi_{equilib}(x)$ from the same regions are

$$(9) \qquad H_{11} = H_{equilib}^{I-I} = \left\langle \Psi_{equilib}^{I} | H | \Psi_{equilib}^{I} \right\rangle = H_{22}$$

According to the general principals of quantum mechanics, the amplitude of C_i states, which previously were constants, begin to depend on time. This is described by the linear system of differential equations [8]

$$(10) \qquad \begin{aligned} i\hbar \frac{dC_1}{dt} &= H_{11}C_1 + H_{12}C_2 \\ i\hbar \frac{dC_2}{dt} &= H_{21}C_1 + H_{22}C_2 \end{aligned}$$

where C_1, C_2 are the state amplitudes $\Psi^I_{equilib}(x)$ and $\Psi^{II}_{equilib}(x)$, respectively.

Once summing up and once subtracting the sides of the above differential equations we get two separated, easy to solve differential equations. Omitting the technical details we get finally

$$(11) \quad \begin{aligned} C_1(t) &= \exp\left(-\frac{iH_{11}t}{\hbar}\right)\cos\left(\frac{H_{12}t}{\hbar}\right) \\ C_2(t) &= \exp\left(-\frac{iH_{11}t}{\hbar}\right)\sin\left(\frac{H_{12}t}{\hbar}\right) \end{aligned}$$

The amplitude C_1 decreases with time as the cosine function and reaches the value zero after $T = (\pi\hbar/2H_{12})$ while C_2 increases as sine function and reaches the value 1 for the same time T. In other words the helium atom moved from the region I to region II after time T. The rate $\nu = 1/T$ also determines the quantum diffusion coefficient D [10]. For a crystal with cubic symmetry one has

$$(12) \quad D = \frac{z}{6}(2d)^2\nu$$

where z is the number of neighbouring interstitial sites and $2d$ is the distance between two sites.

Diffusion of helium atoms in the perfect lattice of UO_2 and ThO_2

The above described solution of the Schrödinger Eq. (5) for the real potential $V(x)$ in the case of the crystal field of UO_2 and ThO_2, allows to determine the matrix elements H_{12}, and thus calculate the diffusion coefficients depending on the height and shape of the potential barrier. The calculation results are shown in Fig. 4. The potential barrier for UO_2 is higher than for ThO_2.

In this figure are shown also the results of measurements, using $^3He(d,\alpha)^1H$ Nuclear Reaction Analysis Technique (see points ▲, ●, ■ and ★ in Fig. 4). Using the values of the potential barrier height, calculated by molecular dynamic methods and reported in [9, 11, 18] and assuming that the shape of the barrier is the same
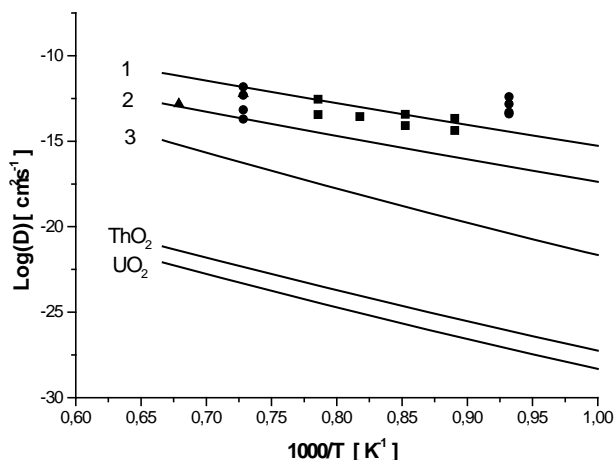

Fig. 4. Temperature dependence of the helium diffusion coefficient in ThO_2 and UO_2 within the Arrhenius range. ThO_2 and UO_2 curves – dependence obtained in this work, 1, 2, 3 – calculated according to the height of the barrier, given by [11, 18], ▲,●,■,★ – experimental values of diffusion coefficients obtained successively in [13, 15–17].
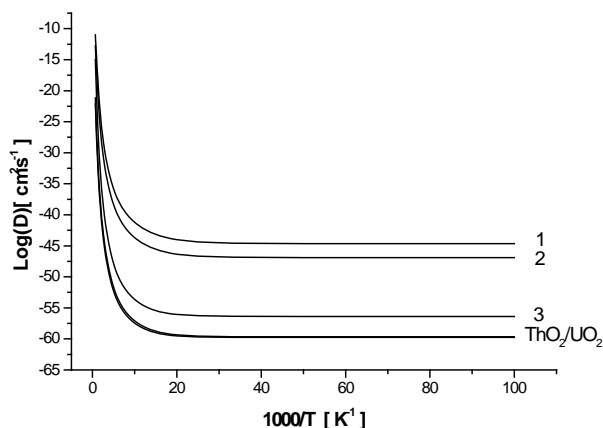

Fig. 5. Temperature dependence of the helium diffusion coefficient in ThO_2 and UO_2 in wide (1500÷50 K) temperature range. Markings as in Fig. 3.

as in Fig. 2, we calculated the diffusion coefficients for these potentials. This time, the experimental points, obtained in [9, 18] lie below the theoretical dependencies. This is not surprising, because the samples used for measurement, inevitably had to include a lot of defects, all the more so that the implantation method used is conducive to the formation of a large amount of structural defects.

On the basis of the measured values of diffusion coefficient at high temperatures, the authors [16] have estimated its value at room temperature for 10^{-37} cm²·s⁻¹. Figure 5 shows the same dependence of diffusion coefficient, but in a wide temperature range. According to our calculations its value for the potential barrier 4.15 eV at 300 K should be in the case of a perfect crystal without defects about 10^{-48} cm²·s⁻¹.

In a further drop in temperature to absolute zero, it should strive asymptotically to about 10^{-60} cm²·s⁻¹, but not to zero, as it would appear from the classical model of diffusion. A similar temperature dependences of the diffusion coefficient were observed by us for the first time experimentally (using Mössbauer spectroscopy method) during migration at low temperatures the interstitial carbon in α-iron [4]. This phenomenon is characteristic of quantum diffusion, which was shown by us in [5, 6].

Discussion

In the case when the helium atom occupies already the octahedral interstitial position, in order to get out of the crystal the atom have to make many over-barrier jumps. Possibility of such a jump, which is one of the channels of diffusion, will depend primarily on the height of the potential barrier. In a perfect lattice, diffusion coefficient should be smaller than in the actually measured samples, which always contain defects, facilitating diffusion. Taking as the starting point the experimental diffusion coefficient values that lie at the lowest in Fig. 4, we obtain a barrier height value which must be greater than 2.56 eV. Thus, the values 2.3 and 2.56, obtained in [9, 18] should be excluded. The value of 3.8 eV, obtained in [11] is equally likely as currently received by us and equal to 4.15 eV. In [11], a semi-classical method – a single Lennard-Jones potential

– was used for calculations while our calculations were made using the "ab initio" method, which is usually more accurate. About the final value of the barrier, only the future experiment can decide, carried out on samples with a minimum content of defects.

Minerals of uranium and thorium dioxide are aged under natural conditions over millions of years at temperatures much lower than obtainable in the laboratory. They should contain a minimum amount of defects. It is expected that the value of the effective potential barrier in the minerals will be close to those obtained by our values.

Helium atoms resulting from the radioactive decay as α particles have the energy thousands of times greater than the ~ 4 electron volts barrier and can easily move in the crystal occupying free octahedral interstitial positions. The old mineral materials containing fissile isotopes hold fairly a lot of noble gases.

These gases are not released during hundreds of millions of years from the old materials, e.g., the mineral thorianite at least 500 000 000 years old occurring in Ceylon contains as much as 10 cm^3 He/g, which is equivalent to the fission gas concentration at a burn-up of 300 000 MWd/t [14].

Conclusions

Helium atom located in the octahedral interstitial position of perfect crystal lattice fcc UO_2 and ThO_2 are submitted to strong repulsive forces from the surrounding metal and oxygen atoms, which means that it is in a deep potential well of depth equal to 4 eV preventing it from any movement in the crystals even at very high temperatures reaching thousands K. Thus the octahedral interstitial positions in thorium dioxide, and even more in uranium dioxide, are effective traps for helium atoms. The trapped helium there immobilized, may stay in the crystal arbitrarily long time. This is supported by the old minerals, where alpha decay occurs, such as thorianite or uraninite which hold fairly a lot of helium during hundreds of millions of years and which could exist in a certain geological period where temperature was very high.

Diffusion of helium in uranium dioxide and thorium dioxide has the character of the quantum leap the barrier potential. While lowering the temperature to absolute zero diffusion coefficient does not tend to zero but to a finite value, equal to about 10^{-60} $cm^2 \cdot s^{-1}$.

The α particles occurring during radioactive decay have a large enough energy to penetrate the crystal and to occupy the octahedral interstitial positions – incorporation process into the crystals.

References

1. Beauvy M (1992) Nonideality of the solid solution in (U, Pu)O_2 nuclear fuels. J Nucl Mater 188:232–238
2. Blaha P, Schwartz K, Madsen G, Kvasnicka D, Luiz J (2001) Wien2k an augmented plane wave plus local orbital program for calculating crystal properties. Vienna University of Technology, Vienna
3. Crocombette JP (2002) "Ab initio" energetic of some fission products (Kr, I, Cs, Sr and He) in uranium dioxide. J Nucl Mater 305:29–36
4. Dąbrowski L (2000) Statics and dynamice of self-ordering alloys. MGU, Moscow (in Russian)
5. Dąbrowski L, Andreev A, Georgiev M (2006) Carbon diffusion in α-iron: Evidence for quantum mechanical tunneling. Met Mater Trans A 37;7:2079–2084
6. Dąbrowski L, Andreev A, Georgiev M (2006) The quantum diffusion of carbon in α-iron in low temperature. Nukleonika 51;2:93–99
7. Dąbrowski L, Szuta M (2012) "Ab initio" study of helium atoms immobilization in UO_2 crystals. Nukleonika 57;3:337–343
8. Feynman RP, Leighton RB, Sands ML (1974) The Feynman lectures on physics. Vol. III. Państwowe Wydawnictwo Naukowe, Warsaw, pp 125–130
9. Govers K (2008) Atomic scale simulations of noble gases behaviour in uranium dioxide. PhD Thesis, ULB-SCK CEN, Bruxels
10. Grabert H, Schober HR (1997) Theory of tunneling and diffusion of light interstitials in metals. Chapter 2. Topics in applied physics. Vol. 73. Springer, Berlin
11. Grimes RW, Miller RH, Catlow CRA (1990) The behaviour of helium in UO_2: Solution and migration energy. J Nucl Mater 172:123–125
12. Gryaznov D, Heifets E, Kotomin E (2009) "Ab initio" DFT+U study of He atom incorporation into UO_2 crystals. Phys Chem Chem Phys 11:7241–7247
13. Guilbert S, Sauvage T, Garcia P et al. (2004) He migration in implanted UO_2 sintered disks. J Nucl Mater 327;2/3:88–96
14. Lewis WB (1964) Engineering for the fission gas in UO_2 fuel. Nucl Appl 2:171–181
15. Martin G, Garcia P, Labrin H et al. (2006) A NRA study of temperature and heavy ion irradiation effects on helium migration in sintered uranium dioxide. J Nucl Mater 357:198–205
16. Roudil D, Deschanels X, Trocellier P, Jegou Ch, Peuget S, Bart J-M (2004) Helium thermal diffusion in a uranium dioxide matrix. J Nucl Mater 325:148–158
17. Trocellier P, Gosset D, Simeone D et al. (2003) ^{3}He thermal diffusion coefficient measurement in crystalline ceramics by µnra depth profiling. Nucl Instrum Methods Phys Res B 210:507–512
18. Yakub E, Ronchi C, Staicu D (2010) Diffusion of helium in non-stoichiometric uranium dioxide. J Nucl Mater 400;3:189–195